Enabling Higher-Order Modulation for Underwater Backscatter Communication

Sayed Saad Afzal, Reza Ghaffarivardavagh, Waleed Akbar, Osvy Rodriguez, Fadel Adib
Massachusetts Institute of Technology
Cambridge, USA
{afzals,rezagh,wakbar,osvyrd,fadel}@mit.edu

***Abstract*—Piezo-acoustic bacskcatter (PAB) is a recently-introduced ultra-low-power underwater communication technology. In contrast to traditional underwater acoustic modems, which need to generate power-consuming carrier signals, PAB nodes communicate by simply reflecting (i.e., backscattering) existing acoustic signals in the environment. This reflection-based approach enables them to communicate at net-zero power but also imposes significant constraints on their throughput and modulation schemes.**

We present *PAB-QAM*, the first underwater backscatter design capable of achieving higher-order modulation. *PAB-QAM* exploits the electro-mechanical coupling property of piezoelectric transducers to modulate their reflection coefficients. Specifically, by strategically employing reactive circuit components (inductors), we demonstrate how *PAB-QAM* nodes can modulate the phase and amplitude of acoustic reflections and realize higher-order and spectrally-efficient modulation schemes such as QAM.

We designed and built a prototype of *PAB-QAM* and empirically evaluated it underwater. Our empirical evaluation demonstrates that *PAB-QAM* can double the throughput of underwater backscatter without requiring additional power, spectrum, or cost. Looking ahead, such increased throughput paves way for various subsea IoT applications in ocean exploration, underwater climate monitoring, and marine life sensing.

***Index Terms*—Subsea IoT, Backscatter Communication, QAM, Piezoelectricity, Wireless, Energy Harvesting, Battery-free**

I. Introduction

The subsea internet-of-things (IoT) has emerged as a new frontier for innovation in real-time ocean monitoring, exploration, and utilization [1]–[4]. Unlike traditional underwater wireless systems that rely on point-to-point communication links between acoustic modems, subsea IoT systems are expected to encompass networks of hundreds to thousands of wireless nodes distributed over wide areas of the ocean [5]. Such networks could transform ocean systems and research by enabling real-time and distributed sensing and monitoring.

While recent research has made important steps toward the vision of a subsea IoT, existing systems still cannot deliver on the power, cost, and throughput requirements of many underwater sensing applications. On the one hand, state-of-the-art low-power acoustic modems can achieve throughputs of 10-100 kbps by adopting complex modulation schemes; these schemes enable transmitting rich sensor data, including underwater images [6]. However, such modems require 50-100 Watts of power for transmissions [7], which quickly drains their batteries of underwater sensors. On the other hand, recent proposals in underwater backscatter can communicate at extremely low power – *sub-milliWatt*s. As a result, they can be deployed for extended periods of time without requiring any batteries. However, these designs are fundamentally limited in their throughput, typically to 1-3 kbps [3], because they rely on very simple modulation schemes. This prevents them from supporting throughput-demanding ocean applications such as imaging marine animals and coral reefs.

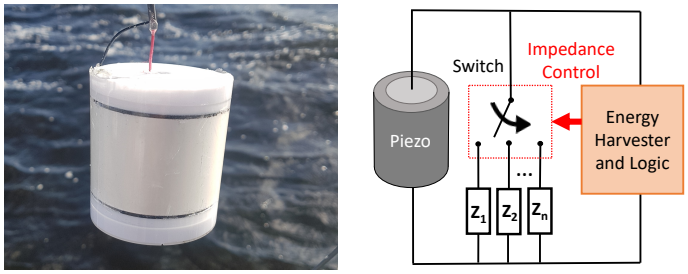

(a) Underwater Backscatter Node (b) Higher-Order Modulation

Fig. 1. ***PAB-QAM*.** (a) shows one of our potted *PAB-QAM* transducers (b) shows the schematic design for *PAB-QAM*.

In this paper, we ask the following question: *Can we bring higher-order modulation to underwater backscatter sensors while maintaining their battery-free nature?* A positive answer to this question would allow us to achieve higher throughput while maintaining the ultra-low-power and low-cost nature of backscatter communication.

To understand the difficulty in achieving higher-order modulation with underwater backscatter, let us first briefly describe how existing backscatter sensors operate. These sensors differ from traditional communication modems in that they do not expend their own energy for transmission. Instead, they communicate by modulating the reflections of existing underwater acoustic signals. Specifically, they transmit bits of '0' and '1' by switching between reflective and non-reflective states. A remote receiver can sense these acoustic reflections to decode the transmitted packets from the backscatter node.[1]

While the backscatter approach described above enables ultra-low-power communication, it suffers from limited modulation capabilities. In particular, existing underwater backscat-

[1]Note that such reflections can be omnidirectional. Moreover, backscatter nodes apply a code on their transmissions, thus enabling a receiver to use this code in order to isolate their packets from other unmodulated reflections in the environment.

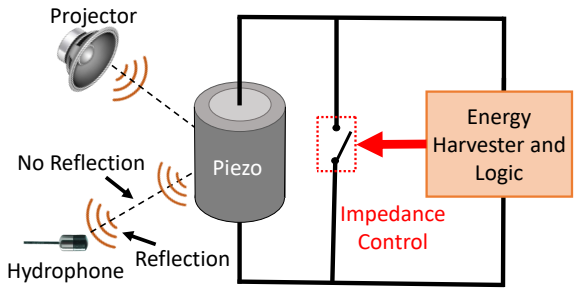

Fig. 2. **Underwater Backscatter.** The figure depicts the operation principle of underwater backscatter communication.

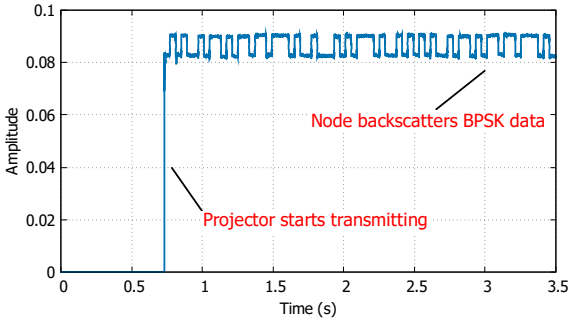

Fig. 3. **Backscattered BPSK Signal.** The figure plots the amplitude of the BPSK backscattered signal as a function of time.

ter nodes, like that shown in Fig. 1(a), can alternate between only *two* reflective states. This can be done by toggling a switch (transistor) on and off between the two terminals of their piezoelectric transducer (as shown in the figure). As a result, they cannot realize higher-order modulation schemes like QAM (Quadrature Amplitude Modulation) which require modulating both the phase and the amplitude of their transmissions. Unfortunately, this limitation has prevented prior designs from achieving higher throughputs via higher-order modulations.

We present *PAB-QAM*, the first underwater backscatter sensor design capable of higher-order modulation. *PAB-QAM* exploits the electro-mechanical coupling property of piezo-electric transducers in order to achieve complex reflection coefficients and realize a larger number of reflection states. Fig. 1(b) shows the schematic of our design for *PAB-QAM*, which consists of a piezo-electric transducer connected to a multi-load switching network. At a high level, the system is able to achieve multiple reflection states by toggling between different complex load impedances Z_i connected between the terminals of the backscatter sensor node. Specifically, the electrical impedance of the load determines the vibration amplitude and phase of the piezo-electric resonator (i.e. reflection). A receiver can sense these different reflection states and use them to decode the transmitted messages. Hence, by enabling more than two reflection states, this design allows us to transmit multiple bits per symbol, thereby achieving higher throughput than prior underwater backscatter designs.

In the rest of this paper, we describes the theoretical and practical aspects of the design and implementation of *PAB-QAM*. We also present an empirical evaluation that demonstrates how our approach can double the throughput of underwater backscatter communication, thus paving way for richer sensing applications in the context of subsea IoT.

II. System Design

A. Primer on Underwater Backscatter

Before delving into our proposed solution to achieve higher-order modulation, let us explain the principles of backscatter communication and how it enables batteryless communication in underwater environments. Below, we briefly describe this principle and refer the interested reader to [3] for more details.

Underwater backscatter systems typically consist of a projector, a hydrophone receiver, and a network of batteryless nodes. For simplicity, let us focus on a single backscatter node, as shown in Fig. 2. The projector transmits an acoustic signal on the downlink. The backscatter node harvests energy from the downlink signal to power up, and it communicates by modulating the reflections of impinging acoustic signals. A remote hydrophone can sense these reflections and use them to decode the transmitted packets from the backscatter node.

In order to harvest energy and modulate acoustic reflections, underwater backscatter nodes rely on piezoelectric resonators. Piezoelectric materials transform sound into electrical energy, enabling these sensors to harvest energy and power up. Once powered up, they can modulate their acoustic reflections by changing the impedance across the terminals of the piezoelectric transducer. Prior designs change this impedance by simply toggling a switch between the terminals of the piezoelectric resonator. By switching between reflective and non-reflective states, they can communicate bits of zero and one.

Fig. 3 shows the received signal by a hydrophone in one of our experimental trials. The figure plots the amplitude as a function of time. At around 0.75s, the amplitude jumps because the projector starts transmitting. Shortly thereafter, we can see that the received signal starts alternating between two amplitudes, corresponding to the two reflective states of the backscatter node. The hydrophone can map these amplitude changes to bits of zero and one, and use them to decode the packets transmitted by a backscatter node. This standard backscatter modulation scheme is inherently limited to only two reflection states.

B. Enabling QAM Backscatter

So far, we have described how standard underwater backscatter systems work. Next, we describe how *PAB-QAM* builds on these prior designs to achieve higher-order modulation. Recall that the challenge in achieving higher-order modulation is that existing underwater backscatter systems can only switch between two states, reflective and non-reflective. However, in order to achieve higher-order modulation, one needs to be able to switch between more states.

To overcome this challenge and realize a larger number of reflection states, *PAB-QAM* exploits the electro-mechanical

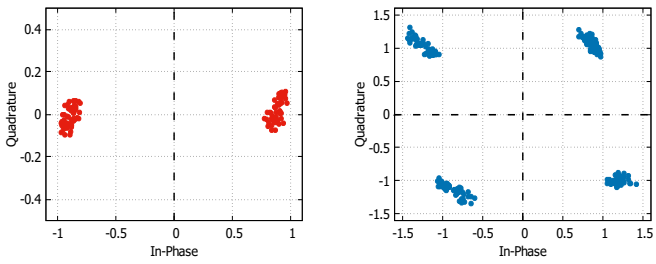

(a) BPSK Backscatter (b) QAM Backscatter

Fig. 4. **Backscatter Constellation.** This figure plots the constellation points of the received backscatter signal for: (a) BPSK backscatter, and (b) *PAB-QAM*.

coupling properties of piezoelectric transducers. Specifically, the reflection properties of a piezoelectric material are determined both by the material itself (and geometry), and by the electrical load connected to it. In particular, due to the coupling between the electrical and mechanical components of piezoelectric materials, changing their electric loads would result in changing the amplitude and phase of their vibration. Since each vibration mode results in a different reflection state, this allows us to encode more than two types of symbols (i.e., more than 1 bit/symbol). Interestingly, the reflective (closed switch) and non-reflective (open switch) states of prior underwater bacskcatter designs correspond to two special cases of this interpretation, where the load impedance is 0 and ∞ respectively.

Mathematically, we can describe the backscatter signal as a function of the reflection coefficient Γ. The reflection coefficient itself can be expressed as a function of the source impedance Z_s (i.e., that of the piezo) and load impedance Z_l (i.e., that of the electrical load) through the following equation:

$$\Gamma = \frac{Z_l - Z_s^*}{Z_l + Z_s^*} \tag{1}$$

Since the source impedance Z_s is constant for a given carrier frequency, we need to modify the load impedance Z_l to obtain different reflection coefficient values. This can be done by choosing reactive components (e.g., inductors) as impedance loads. Fig. 1(b) shows how such a design can be realized in practice by having a switch that can toggle between unique reactive loads.

The above description demonstrates how one can achieve random backscatter reflection states. In practice, we would like to strategically choose these states to achieve high spectral efficiency and high modulation depth (i.e., to separate the reflection coefficients in order to increase their resilience to noise). To make this more concrete, we ran an experiment using a prior (open-close) backscatter design [3]. Fig. 4(a) plots the constellation of the received symbols in the I/Q plane. The plot shows that the received clustered are diametrically opposite at +/-1. This matches the expected constellations from standard BPSK modulation.

When adopting higher-order modulations, we would like to similarly separate the symbols from each other by the maximum possible distance in the I/Q plane. Such separation can typically be achieved by implementing higher-order modulation schemes like Quadrature Amplitude Modulation (QAM) [8]. Thus, we strategically chose the inductor values of the impedance loads in our implementation such that they resulted in QAM constellations. Then, we ran an experiment with a *PAB-QAM* node, and we plot the constellation of the received symbols in Fig. 4(b). The plot shows *PAB-QAM* can indeed encode four different symbols spanning the four quadrants of the I/Q plane – i.e QAM. Thus, it can assign two bits to each symbol (reflection state), which in turn allows it to achieve twice the throughput compared to standard underwater backscatter systems, as we demonstrate empirically in IV.

Few additional points are worth noting:

- So far, our discussion has focused on the implementation of QAM by using multiple complex loads. In principle, this same idea can be extended to achieve other high-order modulation schemes such as PAM, PSK, 16-QAM, etc.[2]
- An alternative way to achieve higher throughput is to increase the switching/backscatter rate. However, such an approach may be less desirable for multiple reasons: first, backscattering at a higher rate would consume more energy because the oscillator would need to run at a higher frequency. Second, higher backscatter rate would require larger bandwidth; however, since piezo-transducers are typically narrow-band, this would result in lower SNR (signal-to-noise ratio). Finally, since the underwater channel is frequency-selective, spreading the signal over a wider bandwidth would complicate the decoding process [10], [11]. Despite these drawbacks, one might still want to adopt higher rates for certain data-intensive applications. In such scenarios, one can combine *PAB-QAM* with recent ultra-wideband underwater backscatter designs [12] as two complementary mechanisms to boost throughput.
- Finally, it is worth noting that our above discussion has ignored the impact of the channel on the constellations. In practice, one can estimate and invert the channel using standard channel estimation techniques from the communication literature [8]. This is typically done by transmitting a training sequence in the preamble p_n, and estimating the channel h from the received signal y_n as follows:

$$h = \sum_n y_n . p_n^* \tag{2}$$

Once the channel is estimated, it can be used to decode the payload of the packet.

[2]It is worth noting that prior work has demonstratted QAM for RFIDs [9]. *PAB-QAM* is inspired by this line of work and brings higher-order modulation to underwater backscatter.

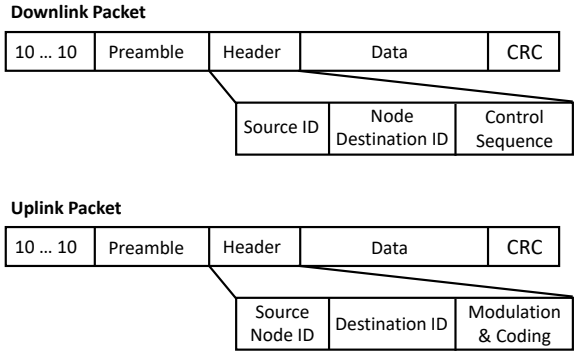

Fig. 5. **Packet Structure.** This figure shows the different fields of the downlink and uplink packet.

C. From Backscatter to Networking

Now that we have discussed how *PAB-QAM* works at the fundamental sensor level, we describe how we can enable networking to scale it to multiple nodes.

Packet Structure: First, we describe the packet structure of underwater backscatter networks. Fig. 5 shows the different components of the uplink (backscatter node to hydrophone) and downlink (projector to backscatter node) packets in *PAB-QAM*. Each packet consists of a preamble, header, payload, and CRC. The preamble contains a training sequence, which is used for synchronization and channel estimation. The training sequence is followed by a header which contains the source ID, node destination ID, and control information. On the downlink, the control sequence may contain a specific time slot or frequency channel for communication. On the uplink, the control sequence is typically the modulation and coding rate of the payload. Note that the preamble and header for the uplink packet is typically in BPSK (or FM0 modulation), while the payload can be in a higher-order modulation scheme. Each packet ends with a CRC sequence which is used to verify if the entire packet was received correctly.

Multiple Access Control (MAC): Our system incorporates a MAC protocol to scale *PAB-QAM* to multiple nodes while minimizing interference. The MAC protocol is arbitrated by the downlink projector. In its simplest form, the projector implements time division multiple access (TDMA) by leveraging the node ID field in the packet header. Specifically, at the beginning of each communication session, the projector can select the node it wishes to communicate with. If multiple backscatter nodes receive the downlink packet, only the node whose ID matches the header field would respond with its sensor data on the uplink, thus avoiding interference. Alternatively, the projector may implement other MAC protocols such as frequency division multiplexing (FDMA) by building on prior work in underwater backscatter [3], [12]. In such scenarios, the projector would use the control sequence field in its downlink packet to assign different frequency channels to different backscatter nodes. Upon decoding the downlink packets, each backscatter node can tune its oscillator to the corresponding frequency channel before starting transmissions.

III. Implementation

In this section, we discuss the implementation of our system, and we elaborate on the different system components and the fabrication process. The implementation of *PAB-QAM* consists of three main components: a backscatter node, acoustic projector, and a receiver.

(a) Backscatter node: We fabricated our backscatter nodes in-house, as shown in Fig. 1(a). Each node consists of a piezoelectric transducer and a hardware controller. To build our transducers, we purchased piezo-ceramic cylinders with a nominal resonance frequency of 17kHz [13]. The fabrication process started by 3D printing the base and cap. Then, we soldered wires to the inner and outer surfaces of the piezo, enclosed the structure with end-caps using a long screw, and placed it inside a mold. Finally, we added polyurethane WC-575A mixture (from BJB enterprise) between the piezo and the mold, and we cured this structure under 4psi pressure using a pressure chamber [14].

The transducer's terminals were connected to a custom-made circuit which is responsible for harvesting energy and controlling the backscatter logic. The circuit uses a rectifier and a super-capacitor to harvest and store electrical energy. Furthermore, this circuit also contains different load impedances which are fine-tuned to get QAM reflections in underwater backscatter. Finally, the circuit includes a MSP430G2553 micro-controller which controls the backscatter logic and switches the load impedance of the backscatter sensor node based on the bits that need to be transmitted [15]. Similar to prior designs in underwater backscatter [3], *PAB-QAM*'s power consumption ranges from 120μW to 500μW.

(b) Acoustic Projector: *PAB-QAM* uses a piezo-ceramic transducer as a projector to transmit a PWM signal on the downlink. This projector is driven by a PDUS210-210W Ultrasonic Driver which is interfaced with a PC using a USB connection [16].

(c) Receiver: The system also uses an omni-directional Reson TC 4014 hydrophone to record the uplink backscatter signal. The hydrophone is connected to N210 USRP which samples the incoming signal and forwards it to a PC using a LAN interface [17]–[19]. The hydrophone's captured signals are processed offline (downcoversion, filtering, and demodulation) in MATLAB for decoding the uplink packets.

IV. Experimental Results

To assess the benefits of higher-order modulation, we evaluated the overall throughput of our proposed design and compared it to prior work in underwater backscatter in both simulations and empirical evaluation.

A. Simulation Results

First, we evaluated the performance of our system in simulation. We simulated its throughput at 521 different SNR values ranging from -15dB to 40dB. At each SNR value, we performed 50 simulation trials, each with random additive white

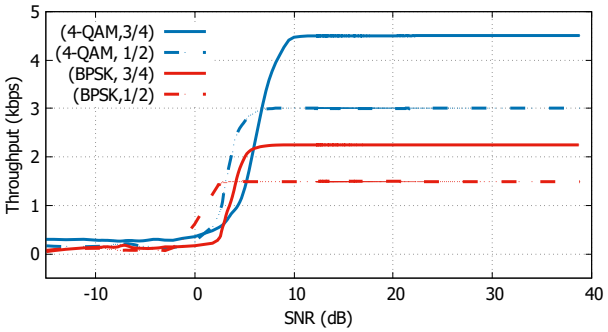

Fig. 6. **Throughput vs SNR (Simulations).** The figure plots the throughput of QAM (blue) and BPSK (red) as a function of SNR with different code rates. For any given code rate, 4-QAM achieves twice the throughput when compared with BPSK.

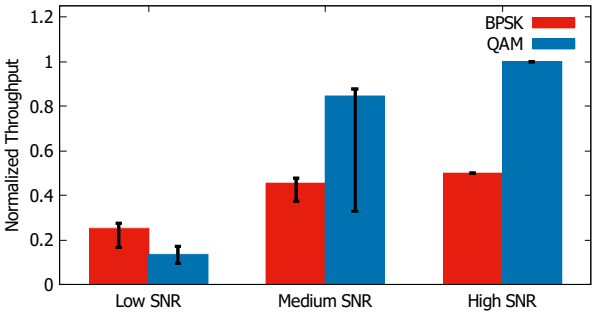

Fig. 7. **Throughput vs SNR (Empirical).** The figure plots the normalized throughput of QAM (blue) and BPSK (red) as a function of SNR. The error bars represents the 25^{th} and 75^{th} percentile respectively.

gaussian noise (AWGN). For each SNR value, we averaged the throughput across all simulation trials. We repeated the same evaluation for *PAB-QAM* and PAB (our baseline) and at two coding rates: 1/2-rate and 3/4-rate. Across all these trials, we fixed the backscatter link frequency (oscillator) to 3 kHz.

Fig. 6 plots the throughput as a function of SNR for 4-QAM (in blue) and BPSK (in red). The dashed lines correspond to a 1/2-rate code while the solid lines correspond to 3/4-rate code. We make the following remarks:

- All modulation schemes start from 0 throughput at low SNRs, then increase with SNRs until they reach a plateau. At high SNRs, *PAB-QAM* outperforms the baseline (i.e., BPSK). Specifically, for all SNR values beyond 10dB, *PAB-QAM* achieves twice the throughput compared to prior underwater backscatter modulation schemes at the same rate.
- For certain low SNR values (between 0dB and 5dB), it may more desirable to use BPSK than QAM. This is expected since, at the same power level (SNR), BPSK is more resilient to noise than QAM because it has larger minimum distance between its constellation symbols.

B. Empirical Results

Next, we evaluated our system by performing real world experiments in a controlled underwater environment (a medium-sized water tank). In these experimental trials, the projector was configured to transmit a downlink signal at a carrier frequency of 20kHz, and we measured the throughput of the backscatter node on the uplink. We performed experimental trials at three different SNR regimes: low, medium, and high (representing different SNR regions of Fig. 6). To achieve different SNRs, we changed the location of the backscatter node and/or the power transmitted by the downlink projector. For each configuration (of power and location), we repeated the same experimental trial for both *PAB-QAM* and our baseline (BPSK). We performed 120 trials in total.

Fig. 7 plots the median normalized throughput for both QAM and BPSK as a function of SNR. Specifically, we normalized the throughput by the highest achieved median throughput of *PAB-QAM* at high SNR. The error bars represent the 25^{th} and 75^{th} percentile respectively. We make the following remarks:

- At high SNR, *PAB-QAM* achieves twice the throughput of BPSK. This is expected because higher-order constellations such as QAM allow us to transmit more bits per symbol (i.e. 2 bits instead of 1 in case of BPSK) which increases our throughput by a factor of 2. Moreover, this result matches the expected performance based on our simulations in section IV-A.
- For low SNR values, BPSK achieves slightly higher throughput than 4-QAM. This is also expected (and matches simulations) because BPSK is more resilient to noise since it has larger minimum distance between two adjacent symbols in its normalized constellation.

These results demonstrate the importance of *PAB-QAM*'s ability to achieve higher order modulation. They also show that it may be desirable to incorporate bit rate adaptation schemes in underwater backscatter in order to enable them to gracefully scale their bit rate to channel conditions.

V. Conclusion

This paper presents *PAB-QAM*, the first underwater backscatter design capable of achieving higher-order modulation. This design marks an important step forward in ultra-low-power underwater networking by demonstrating the potential of doubling the throughput of backscatter communication nodes through QAM modulation. As underwater backscatter continues to evolve, we hope that it will pave way for ultra-low-power and low-cost subsea IoT for ocean monitoring, scientific exploration, and marine life sensing.

Acknowledgment

We thank the anonymous reviewers and the Signal Kinetics group for their feedback. This research is supported by the Office of Naval Research, the MIT Media Lab, and the Doherty Chair in Ocean Utilization.

REFERENCES

[1] Rajeswari Jayaraman, "Beyond IoT: Internet of Underwater Things to Network the Oceans," https://www.prescouter.com/2017/06/internet-of-underwater-things/, 2017.

[2] C.-C. Kao, Y.-S. Lin, G.-D. Wu, and C.-J. Huang, "A comprehensive study on the internet of underwater things: applications, challenges, and channel models," *Sensors*, vol. 17, no. 7, p. 1477, 2017.

[3] J. Jang and F. Adib, "Underwater backscatter networking," in *Proceedings of the ACM Special Interest Group on Data Communication*. ACM, 2019, pp. 187–199.

[4] E.-C. Liou, C.-C. Kao, C.-H. Chang, Y.-S. Lin, and C.-J. Huang, "Internet of underwater things: Challenges and routing protocols," in *2018 IEEE International Conference on Applied System Invention (ICASI)*. IEEE, 2018, pp. 1171–1174.

[5] DARPA, "Ocean of Things Aims to Expand Maritime Awareness across Open Seas," https://www.darpa.mil/news-events/2017-12-06, 2017.

[6] J. W. Choi, T. J. Riedl, K. Kim, A. C. Singer, and J. C. Preisig, "Adaptive linear turbo equalization over doubly selective channels," *IEEE journal of oceanic engineering*, vol. 36, no. 4, pp. 473–489, 2011.

[7] WHOI, "WHOI Micro-modem," https://acomms.whoi.edu/micro-modem/.

[8] D. Tse and P. Viswanath, *Fundamentals of wireless communication*. Cambridge university press, 2005.

[9] S. Thomas and M. S. Reynolds, "Qam backscatter for passive uhf rfid tags," in *2010 IEEE International Conference on RFID (IEEE RFID 2010)*. IEEE, 2010, pp. 210–214.

[10] M. Stojanovic and J. Preisig, "Underwater acoustic communication channels: Propagation models and statistical characterization," *IEEE communications magazine*, vol. 47, no. 1, pp. 84–89, 2009.

[11] M. Bae, J. Park, J. Kim, D. Xue, K.-C. Park, and J. R. Yoon, "Frequency-selective fading statistics of shallow-water acoustic communication channel with a few multipaths," *Japanese Journal of Applied Physics*, vol. 55, no. 7S1, p. 07KG03, 2016.

[12] R. Ghaffarivardavagh, S. S. Afzal, O. Rodriguez, and F. Adib, "Ultra-wideband underwater backscatter via piezoelectric metamaterials," in *Proceedings of the Annual conference of the ACM Special Interest Group on Data Communication on the applications, technologies, architectures, and protocols for computer communication*, 2020, pp. 722–734.

[13] STEMINC., "Piezo ceramic cylinder 54.1x47x40mm 17 khz.(2020). part no. smc5447t40111." https://www.steminc.com/PZT/en/piezo-ceramic-cylinder541x47x40mm-17-khz, 2020/, 2020.

[14] B. E. 2015., "Water clear shore 70 s polyurethane elastometer." https://bjbenterprises.com/index.php/wc-575-a-b/, 2015.

[15] "Texas instruments inc. 2019. msp430g2553." http://www.ti.com/product/ MSP430G2553. (2019)/, 2019.

[16] PDUS210., "Pdus210 – 210 watt ultrasonic driver / generator (2020)." https://www.piezodrive.com/ultrasonic-drivers/pdus210-ultrasonic-driver/, 2020.

[17] TELEDYNEMARINE., "Reson tc-4014 hydrophone. part no. tc-4014." https://www.teledynemarine.com/reson-tc-4014/, 2020.

[18] "LFRX daughterboard," http://www.ettus.com, ettus inc.

[19] "usrp n210," http://www.ettus.com, ettus inc.